β-CD-decorated BODIPY-based porous polymer for improved photodegradation

*Xin Wang,[a,†] Wuzi Zhao,[a,†] Shiyuan Zhou,[a] Peiyang Gu,[*a] Hua Sun[*b] and Danfeng Wang[*a,c]*

Supporting Information

CONTENTS

1. Materials and Methods

Infrared spectroscopy

The Fourier Transform Infrared (FT-IR) spectra of the samples were measured using an FT-IR spectrophotometer (Thermo Scientific Co., United States, Nicolet 6700) in the wavenumber range of 4000-400 cm^{-1}, employing the KBr pellet method.

Thermogravimetric analysis

The thermal stability of the materials is measured by thermogravimetric analysis (TGA, TG209F3, Germany) from 40 ℃ to 800 ℃ with a heating rate of 10 ℃ min^{-1}.

N_2 adsorption-desorption isotherms

The N_2 adsorption-desorption isotherms were performed on a Quantachorme Micromeritics ASAP 2020 instrument at 77 K. Based on the N_2 adsorption-desorption data, the Brunauer-Emmett-Teller (BET) method was used to calculate the specific surface area of the samples.

UV-Vis

The optical properties of the samples were characterized using a UV-Vis spectrophotometer (Shimadzu, UV3600) in the wavelength range of 190-1300 nm.

Scanning Electron Microscopy

Scanning electron microscopy images were recorded on an SEM (FE-SEM, SUPRA-55, Germany) with an EHT voltage of 1.2 kV. The sample was slightly ground and distributed onto the surface of an ITO (0.5 cm × 0.5 cm).

Contact angle

The hydrophilicity and hydrophobicity of the catalyst are measured in a contact angle analyzer.

High performance liquid chromatography

The real-time concentration of BPA during degradation was tested by high performance liquid chromatography (HPLC).

Nuclear magnetic resonance spectroscopy

The solid-state ^{13}C NMR was measured on a Bruker 400 MHz NMR spectrometer. Spectra of soluble samples were recorded using a BRUKER AV400TR spectrometer.

Electron spin resonance

An electron spin resonance (ESR) spectrometer (JEOL, JES-X320) detected the signals of active radicals.

Electrochemical measurements

The photocurrent, electrochemical impedance spectroscopy (EIS), and Mott-Schottky analysis of the material were tested by an electrochemical workstation (CHI760E, Shanghai, China). The working electrodes were prepared as follows: 5 mg of polymer catalysts and 10 μL 5 wt% Nafion were generally dispersed in 1 mL of anhydrous ethanol and ultrasonicated for 60 min to form a homogeneous suspension. 60 μL of the obtained suspension was dropped onto the surface of an ITO (1 cm × 2 cm) glass electrode and dried for 30 min in the air at 25 ℃. With 0.1 M Na_2SO_4 aqueous solution supplied as the electrolyte, the Ag/AgCl electrode and platinum wire were the reference electrode and counter electrode, respectively. Meanwhile, the Xe Lamp (300W, Shenzhen Ouying Lighting Science and Technology Co., Ltd.) placed at 20 cm away from the electrolytic cell were employed as the light source. The photocurrents were tested under Xe lamp irradiation with light on-off cycles at a time interval of 30 s and the scan rate was 100 mV s^{-1}. The Mott-Schottky analysis was carried out in the dark. In EIS measurements, the working electrodes was replaced with a glass carbon electrode (60 μL of the obtained suspension was dropped onto the

surface of a glass carbon electrode and dried for 30 min in the air at 25 ℃), with 0.1 M $K_3[Fe(CN)_6]$ aqueous solution as the supporting electrolyte.

2. Synthetic procedures

Chemicals: 4-fluorobenzaldehyde, 2,4-dimethylpyrrole, trifluoroacetic acid, 2,3-dichloro-5,6-dicyanobenzoquinone (DDQ), anhydrous boron trifluoride ether, *N*-iodosuccinimide (NIS), 1,4-diynebenzene, *N,N*-dimethylformamide (DMF), diisopropylamine (DIPA), β-Cyclodextrin (β-CD), Tetrakis(triphenylphosphine)palladium ($Pd(PPh_3)_4$), cuprous iodide (CuI), 2,2-dimethyl-1-oxido-3,4-dihydropyrrol-1-ium (DMPO), triacetonamine (TEMP), *p*-benzoquionone (*p*-BQ), ethylenediaminetetraacetic acid disodium salt (EDTA-2Na), L-histidine, isopropanol (IPA)， sodium chloride (NaCl), sodium nitrate ($NaNO_3$), sodium carbonate (Na_2CO_3), sodium sulfate (Na_2SO_4), potassium carbonate (K_2CO_3), disodium hydrogen phosphate (Na_2HPO_4), and all the solvents were purchased from local supplier. The tetrahydrofuran, dichloromethane (CH_2Cl_2) and triethylamine (Et_3N) were redistilled over calcium hydride (CaH), and other solvents were directly used without further purification.

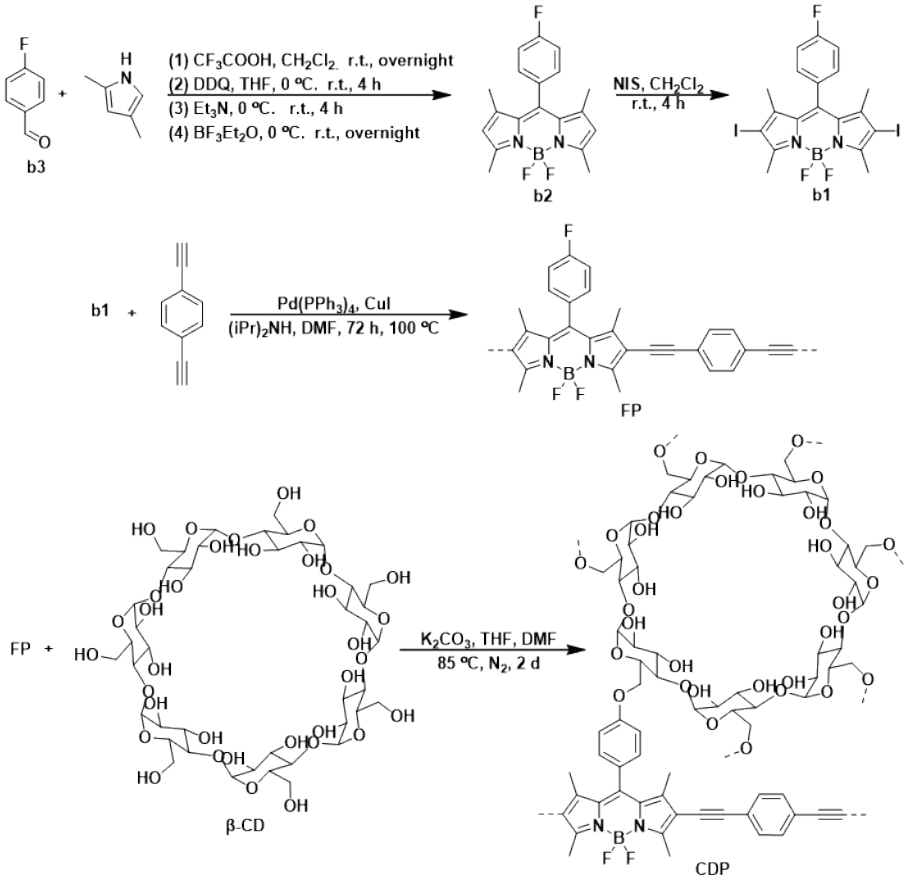

Scheme S1. Synthetic routes of **CDP**.

Synthesis of b2

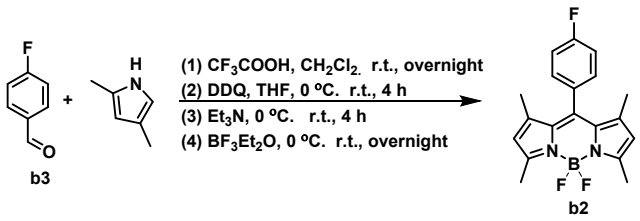

Compound **b2** was synthesized according to a literature procedure with modifications.[1] To a mixture of 4-fluorobenzaldehyde (**b3**, 2.48 g, 20.00 mmol) and 2,4-dimethylpyrrole (3.97 g, 40.00 mmol) in 200 mL CH_2Cl_2, 60 μL of trifluoroacetic acid was added. The mixture was degassed for 30 min and then kept at room temperature under N_2 atmosphere overnight. After the reaction is completed, a mixture of 2,3-dichloro-5,6-dicyanobenzoquinone (4.55 g, 20.00 mmol) in anhydrous tetrahydrofuran (20 mL) was added into the flask slowly under ice condition. The reaction was warmed to room temperature and stirred for 4 h under a nitrogen

atmosphere. 60 mL of anhydrous triethylamine was added into the flask slowly under ice condition. The reaction was warmed to room temperature and stirred for 4 hours under a nitrogen atmosphere. 60 mL of anhydrous boron trifluoride ether was added into the flask slowly under ice condition. The reaction was warmed to room temperature and stirred overnight under a nitrogen atmosphere. The reaction mixture was detected by thin layer chromatography (TLC) until the initial substance was lost. Ice cold saturated sodium bicarbonate solution (200 mL) was poured into reaction mixture to quench the reaction and the organic layer was separated and concentrated under reduced pressure. The crude product was purified by column chromatography on silica gel (CH_2Cl_2 : *n*-hexane = 1: 2, v/v) to give out a dark red solid (2.19 g, 6.00 mmol, Yield = 30%). ^{1}H NMR (400 MHz, Chloroform-*d*): δ = 7.25 (dd, *J* = 8.8, 5.3 Hz, 2H, Ar-H), 7.19 (t, *J* = 8.6 Hz, 2H, Ar-H), 5.97 (s, 2H, py-H), 2.53 (s, 6H, py-CH_3), 1.38 (s, 6H, py-CH_3).

Synthesis of b1

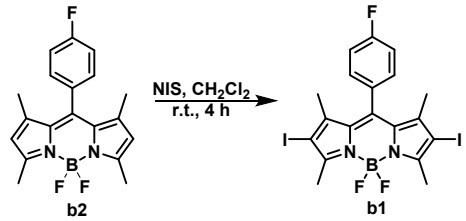

Compound **b1** was synthesized according to a literature procedure with modifications.[2] **b2** (1.00 g, 2.90 mmol) was dissolved in dry CH_2Cl_2 (100 mL), then *N*-iodosuccinimide (NIS, 1.58 g, 7.00 mmol) was added slowly under ice-cold condition. After the addition, the mixture was warmed to room temperature and stirred for 4 hours. The reaction mixture was detected by TLC until the initial substance was lost. The solvent was removed under reduced pressure and the crude product was purified by column chromatography on silica gel (CH_2Cl_2 : *n*-hexane = 1: 2, v/v) to give out an orange red solid (1.64 g, 2.80 mmol, Yield = 96%). ^{1}H NMR (400 MHz, Chloroform-d) δ 7.78 (d, *J* = 8.0 Hz, 2H, Ar-H), 7.46 (d, *J* = 7.9 Hz, 2H, Ar-H), 2.57 (s, 6H, py-CH_3), 1.34 (s, 6H, py-CH_3).

Synthesis of compound FP

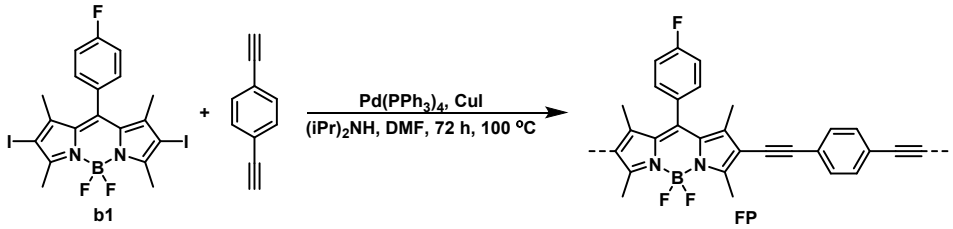

Polymer **FP** was synthesized by the Sonogashira coupling reaction of **b1** and 1,4-diynebenzene. In a 100 mL Schlenk flask, **b1** (100 mg, 0.17 mmol) and 1,4-diynebenzene (21 mg, 0.17 mmol) were dissolved in a mixed solvent of 15 mL DMF and 20 mL DIPA (v/v = 4/3), and the mixture was degassed for 30 min. Then, the catalysts CuI (4 mg, 0.02 mmol) and $Pd(PPh_3)_2Cl_2$ (12 mg, 0.01 mmol) were added. The reaction mixture was purged with N_2 for 30 min before heating at 100 °C for 72 h. After completion, the reaction was cooled to room temperature, and the precipitates were collected by filtration, and washed by DMF (50 mL × 3), THF (50 mL × 3), and CH_3OH (50 mL × 3), respectively. The crude product was followed by Soxhlet extraction with THF, CH_3OH, and CH_2Cl_2, respectively, the solid obtained was then oven-dried at 70 °C overnight to give out a black solid (84 mg, Yield = 70%).

Synthesis of compound CDP

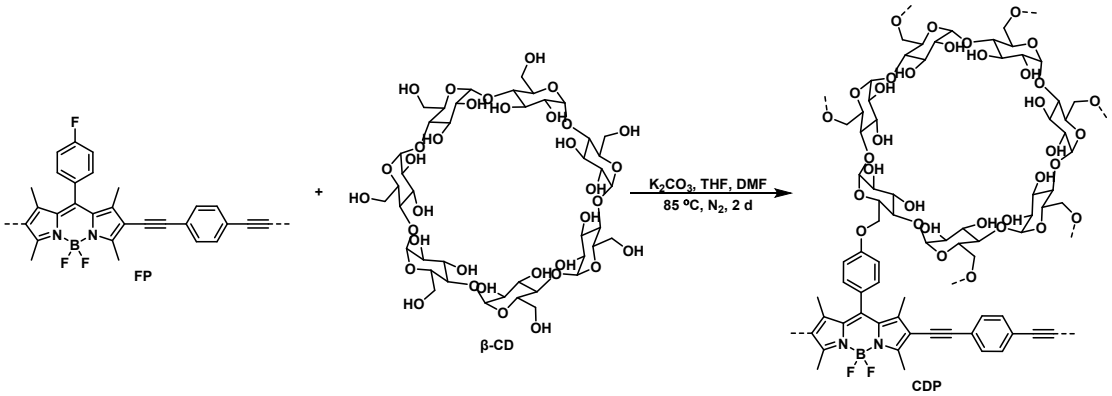

Anhydrous potassium carbonate (2.32 g, 16.80 mmol) was added into a mixture of **FP** (700 mg, 1.40 mmol) and β-CD (795 mg, 0.70 mmol) in a mixed solvent of 20 mL DMF and 100 mL THF in a 250 mL Schlenk flask under N_2 atmosphere. The

mixture was warmed to 85 °C and kept for 2 days. After the reaction, the mixture was filtered and washed with methanol (50 mL × 3). The filtered cake was followed by Soxhlet extraction with THF, CH_3OH, and CH_2Cl_2, respectively; the solid obtained was then oven-dried at 70 ℃ overnight to give out a black-grey solid (1027 mg, yield = 70%).

Characterizations

(1) X-ray diffraction profiles

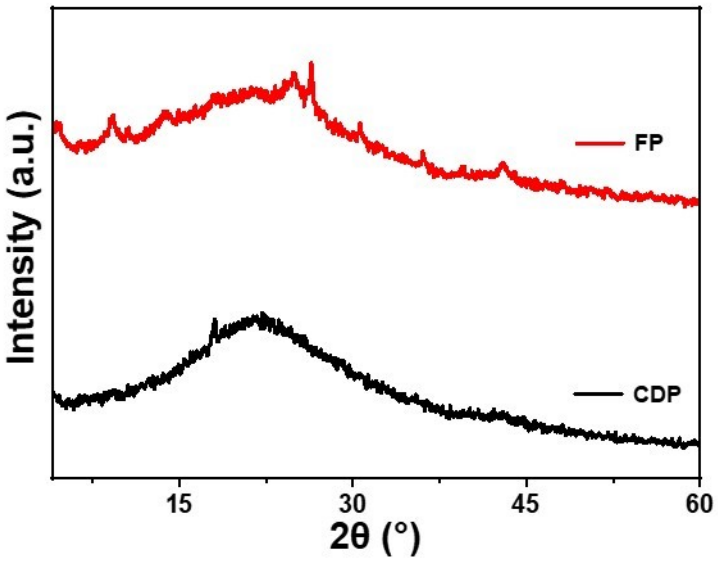

Fig. S1. X-ray diffraction profiles of **FP** and **CDP**.

N_2 adsorption (filled) and desorption isotherm profiles at 77 K

Table S1. The BET surface area related data of **CDP** and **FP.**

Sample	BET surface area S_{BET} (m^2 g^{-1})	Total pore volume (cm^3 g^{-1})	Pore size distribution (nm)
CDP	17.7660	0.046153	9.8187
FP	40.1016	0.136922	13.4695

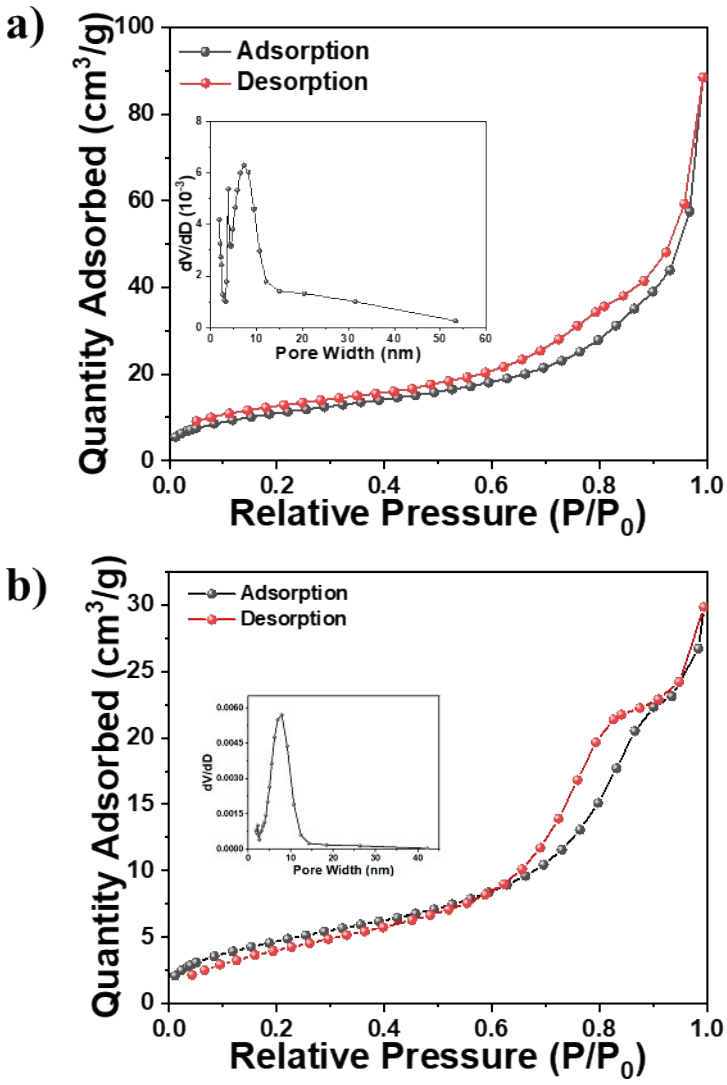

Fig. S2. N_2 adsorption (filled) and desorption isotherm profiles of a) **FP** and b) **CDP** at 77 K.

Fourier-transform infrared (FT-IR) spectra

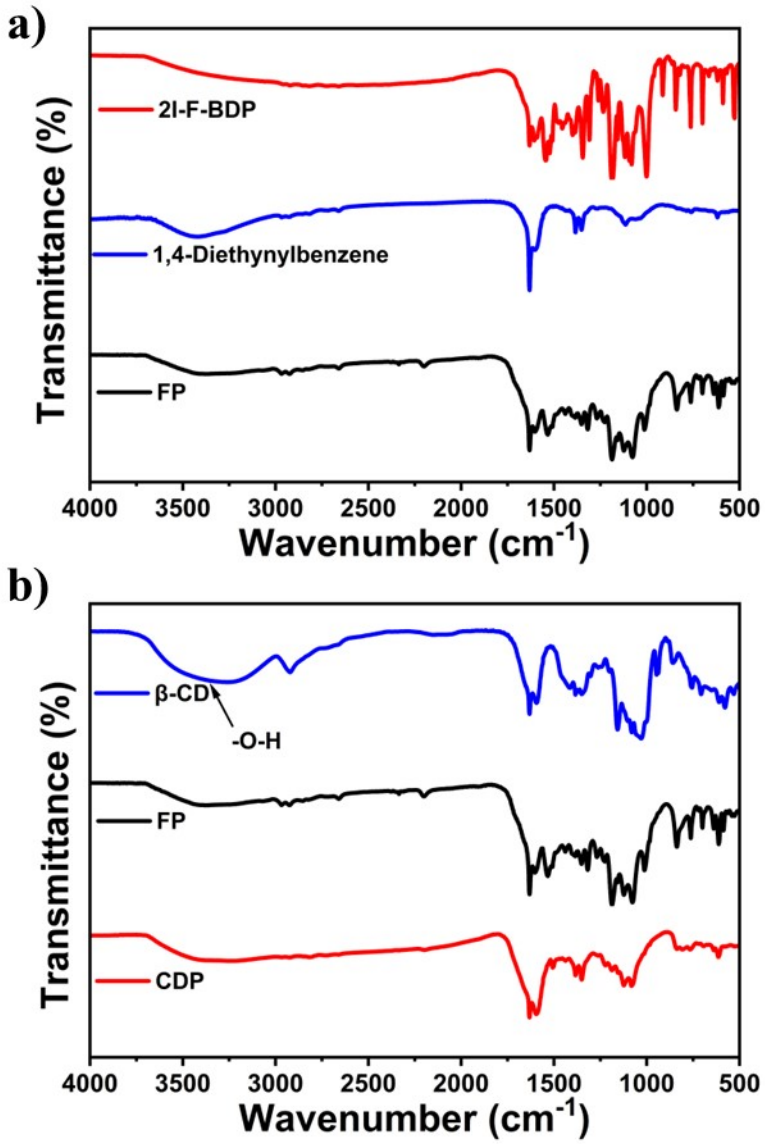

Fig. S3. FT-IR spectra of a) the precursors and b) **CDP**.

X-ray photoelectron spectroscopy (XPS)

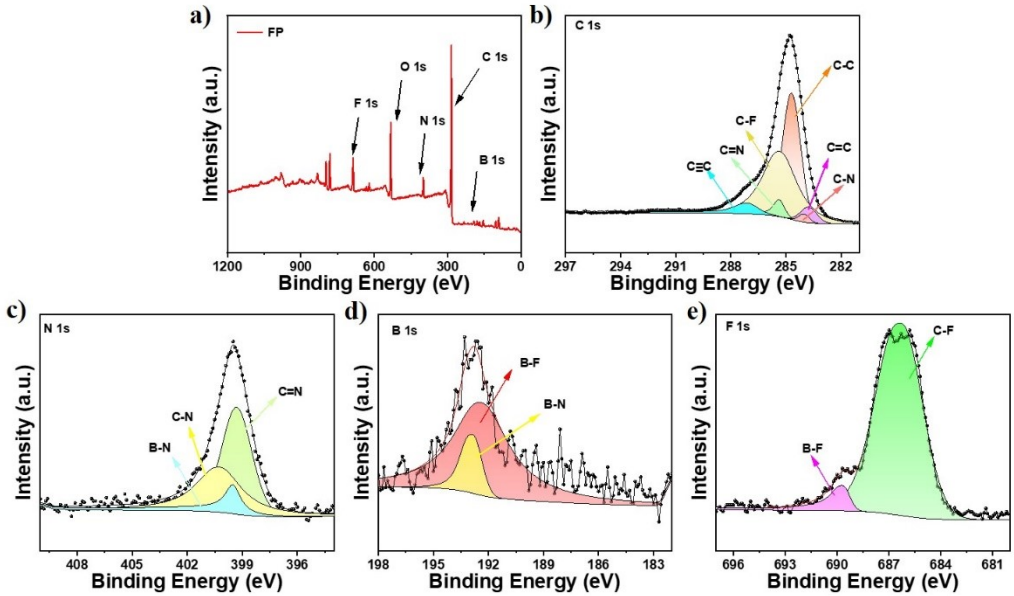

Fig. S4. a) XPS spectra of **FP**. The b) C 1s, c) N 1s, d) B 1s and e) F 1s high resolution XPS spectrum of **FP**.

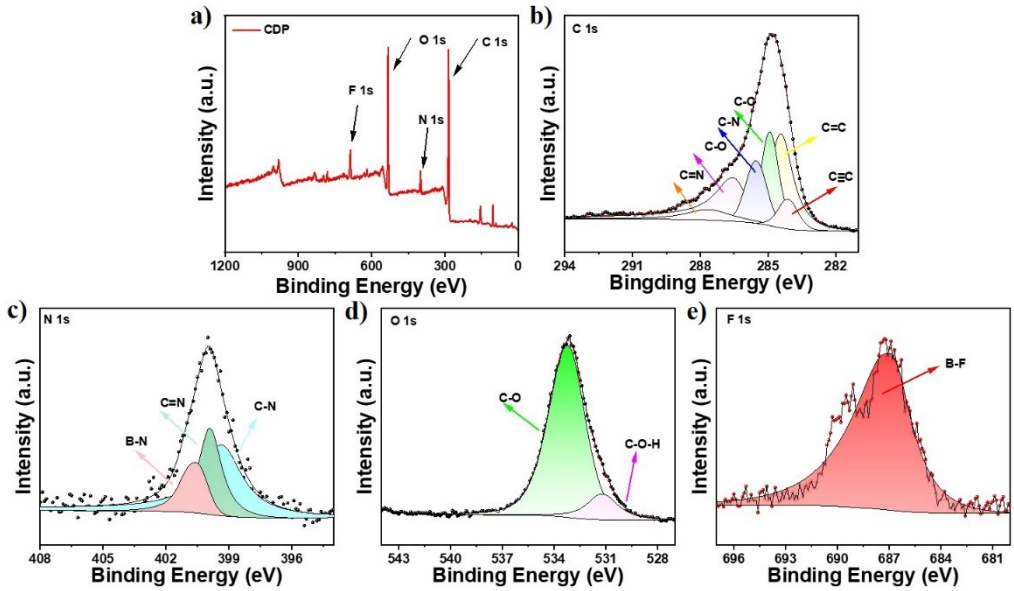

Fig. S5. a) XPS spectra of **CDP**. The b) C 1s, c) N 1s, d) O 1s and e) F 1s high resolution XPS spectrum of **CDP**.

Table S2. XPS data of **FP** and **CDP.**

Core level	Component	Binding energies (eV)	Core level	Component	Binding energies (eV)
FP			**CDP**		
C 1s	C-C	284.80	C 1s	C-C	284.90
	C=C	282.21		C=C	284.11
	C≡C	283.00		C≡C	284.41
	C-N	289.11		C-N	287.57
	C=N	286.92		C=N	285.52
	C-F	291.90		C-O	286.56
N 1s	C-N	399.52	N 1s	C-N	399.62
	C=N	399.31		C=N	399.21
	B-N	400.22		B-N	400.02
B 1s	B-F	192.74	O 1s	C-O	531.18
	B-N	193.80		C-O-H	533.21
F 1s	B-F	686.47	F 1s	B-F	686.98
	C-F	685.50			

Water Contact Angle

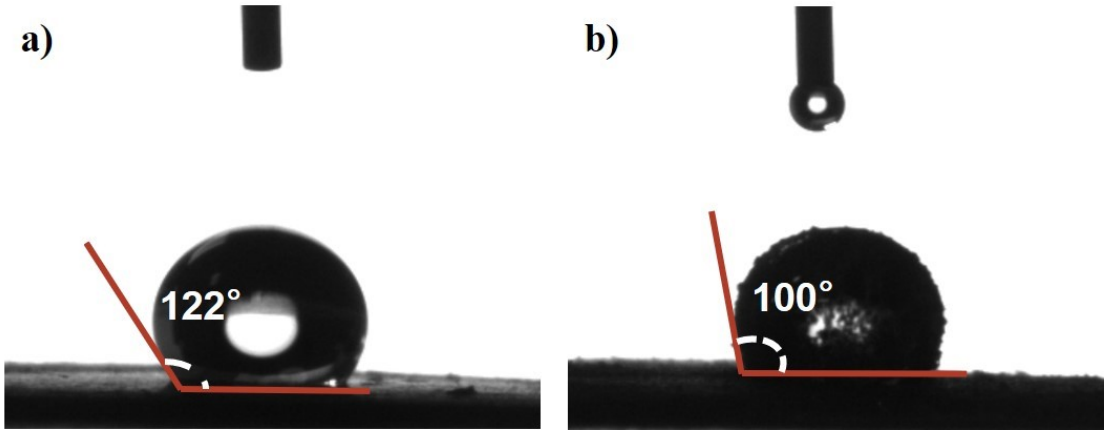

Fig. S6. Water contact angles of a) **FP** and b) **CDP.**

(6) Thermogravimetric analysis (TGA)

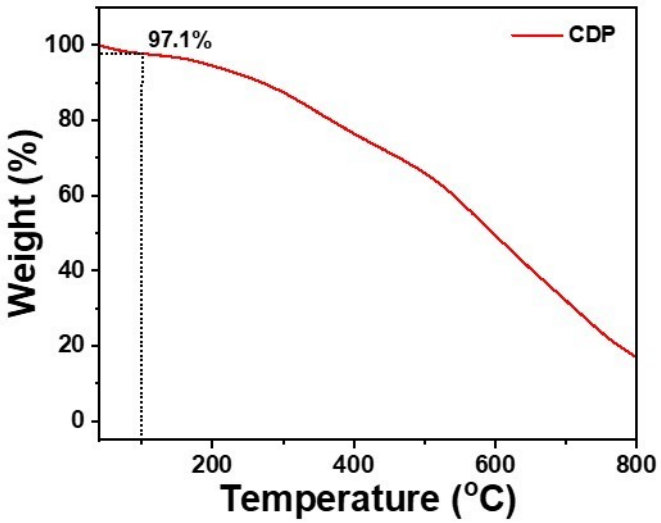

Fig. S7. TGA curve of **CDP.**

(7) Solid-state ^{13}C CP/MAS NMR spectra

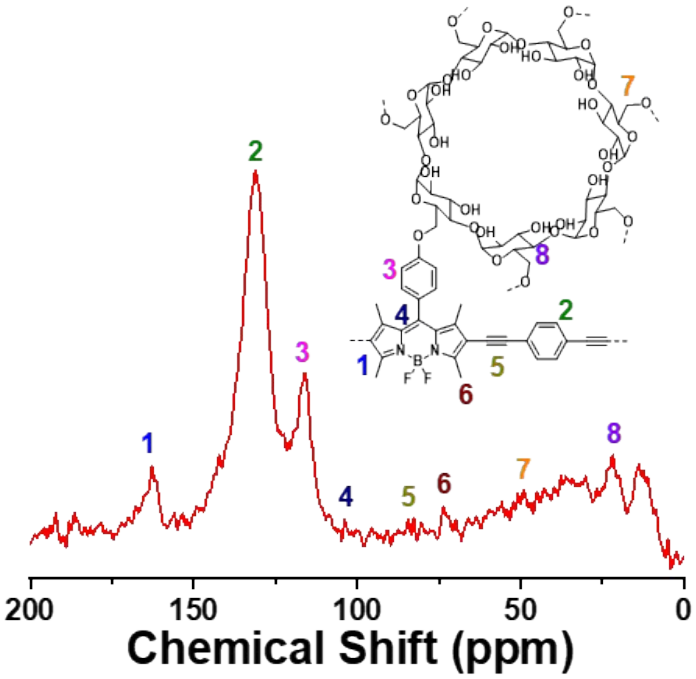

Fig. S8. Solid-state ^{13}C CP/MAS NMR spectra and peak assignments of **CDP.**

3. Adsorption Experiments

Adsorption kinetics

In a typical experiment, 5 mg **CDP** was dispersed in 9.5 mL distilled water and pre-sonicated for 5 min, then it was transferred into a flask and stirred at 600 rpm, 25 ℃. 0.5 mL target pollutants aqueous solutions (200 ppm) was poured into the flask and 1 mL mixture was taken out with an injection syringe at certain time intervals, then immediately passed through a 0.22 μm syringe filter and the filtrate was tested by high performance liquid chromatography.

The adsorption kinetics data of the **CDP** are fitted with pseudo-second-order model and pseudo-first-order model, and the results are shown and summarized in Fig. S9-S10 and Table 1. The adsorption capacity in equilibrium Q_e (mg g^{-1}) and at t time Q_t (mg g^{-1}) is calculated according to eq. S1 and S2:

$$Q_e = \frac{C_i - C_e}{m} V \qquad \text{(eq. S1)}$$

$$Q_t = \frac{C_i - C_t}{m} V \qquad \text{(eq. } S2\text{)}$$

Where m (mg) is the dosage of the adsorbent, V (mL) is the volume of the dyes aqueous solutions, C_t (mg L^{-1}) is the concentration at t time. The pseudo-first-order model is:

$$\ln\left(Q_e - Q_t\right) = \ln Q_e - k_1 t \qquad \text{(eq. } S3\text{)}$$

The pseudo-second-order model is:

$$\frac{t}{Q_t} = \frac{1}{k_2 Q_e^2} + \frac{t}{Q_e} \qquad \text{(eq. } S4\text{)}$$

where Q_t (mg g^{-1}) is the adsorption capacity at t time (min), the k_1 (min^{-1}) and k_2 (g mg^{-1} min^{-1}) are the constants of pseudo-first-order model and pseudo-second-order model, respectively.

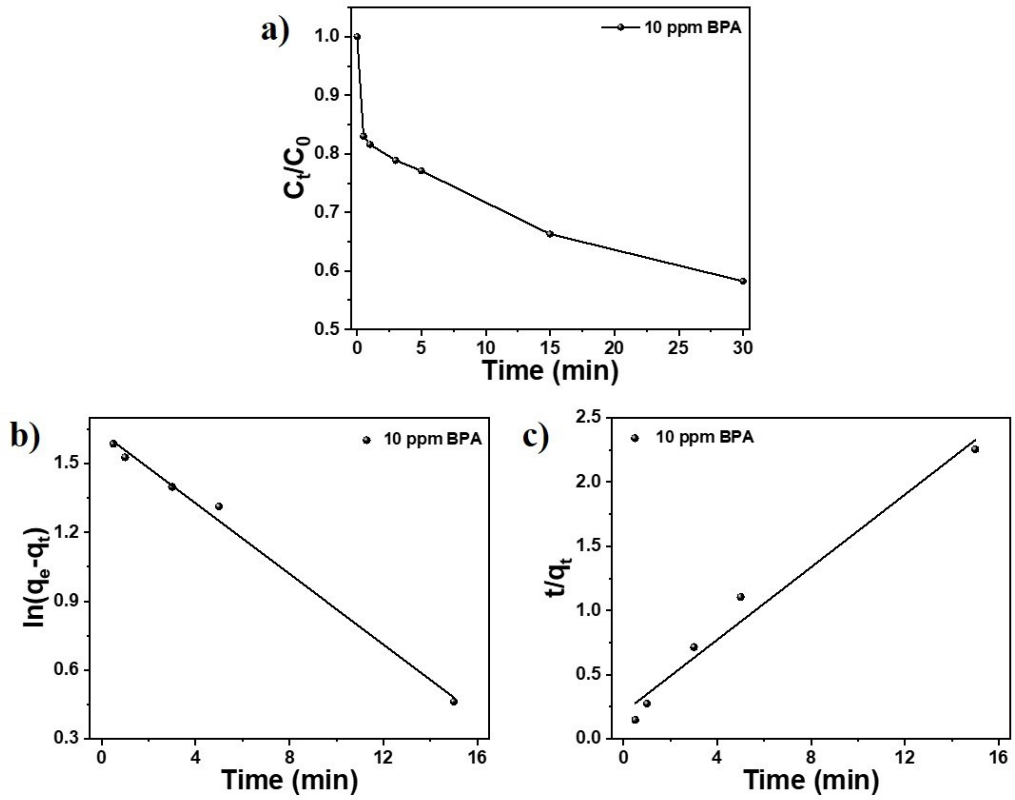

Fig. S9. Kinetic simulation of BPA adsorption onto **FP**. a) adsorption experiments of 10 ppm BPA in the presence of 0.5 mg mL^{-1} of **FP**, b) pseudo-first-order model (10 ppm) and c) pseudo-second-order model (10 ppm).

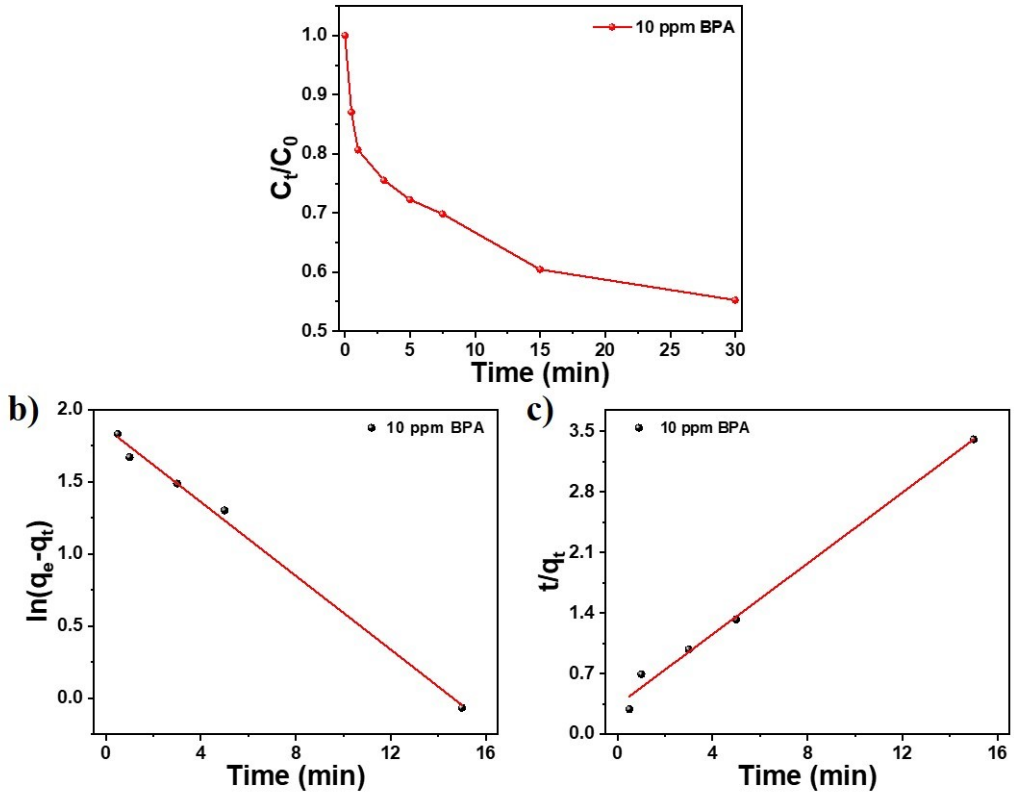

Fig. S10. Kinetic simulation of BPA adsorption onto **CDP.** a) adsorption experiments of 10 ppm BPA in the presence of 0.5 mg mL^{-1} of **CDP**, b) pseudo-first-order model (10 ppm) and c) pseudo-second-order model (10 ppm).

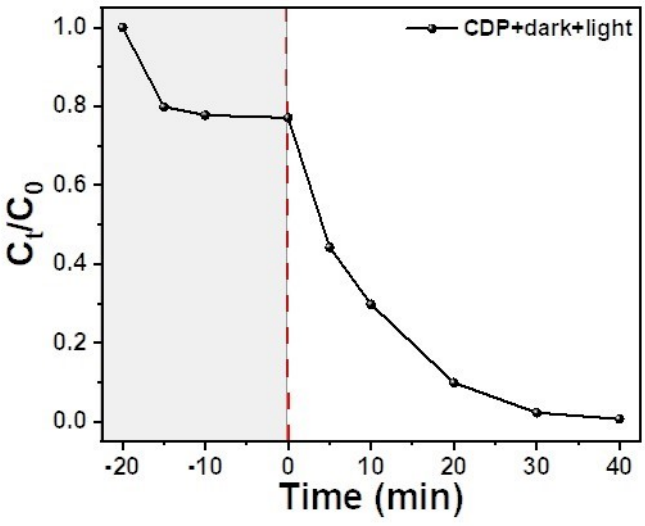

Fig. S11. Adsorption and degradation curve of the catalyst under the sequential condition of 20 min in the dark and 40 min in light.

Adsorption isotherms

The maximum adsorption capacity (Q_m) of **CDP** was calculated in the adsorption isothermal experiments. Firstly, target pollutants and aqueous solutions were prepared with different initial concentrations (0-50 ppm for BPA). Secondly, **CDP** was added into the solutions with the same dosages (0.33 mg mL^{-1}), and then the mixtures were stirred at 600 rpm and 25 ℃ for 48 h. Thirdly, the Q_e was calculated according to eq. S1 and two models, including Langmuir and Freundlich models, were adopted to fit the data of adsorption isotherms.

The Langmuir model is:

$$Q_e = \frac{K_L Q_m C_e}{1 + K_L} \qquad \text{(eq. } S5\text{)}$$

The Freundlich model is:

$$Q_e = K_F C_e^{1/n} \qquad \text{(eq. } S6\text{)}$$

Where K_L and K_F are the constants of the Langmuir model and Freundlich model, respectively; 1/n is the empirical parameter of the Freundlich model.

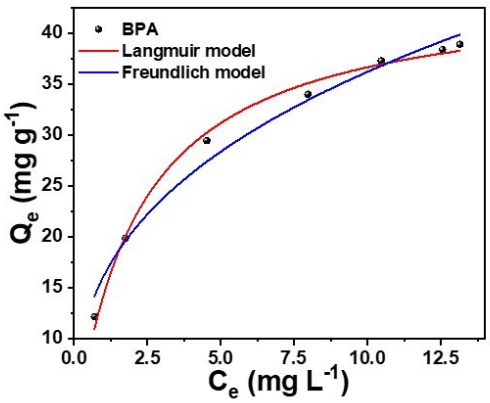

Fig. S12. The fitting diagram of Langmuir models and Freundlich model of BPA.

Table S3. The data of adsorption isotherms of **CDP** towards BPA.

Adsorbents	Pollutants	Langmuir model			Freundlich model		
		Q_m (mg g^{-1})	k_L (L mg^{-1})	R^2	k_F (mg g^{-1})	1/n	R^2
CDP	BPA	44.48	0.469	0.9938	16.0875	0.3527	0.9836

4. Photodegradation Experiments

General procedure for photodegradation of organic pollutants.

The photocatalytic degradation reaction setup consists of a 300 W Xe lamp (MC-PF300C), a 50 mL double-walled beaker, a circulating water system, and a magnetic stirrer (the 50 mL double-walled beaker is used to control the temperature during the photocatalytic process by circulating water).

All the photocatalytic experiments were conducted under the Xe lamp, with a distance of 10 cm between the reactor and the lamp. The photocatalytic reaction was carried out at room temperature, following these steps: firstly, 5 mg of catalyst **CDP** was dispersed in 9.5 mL of ultrapure water using ultrasound for 10 min; then, the dispersed catalyst solution was transferred into the reactor, followed by adding 0.5 mL of a 200 ppm BPA aqueous solution. The reactor was illuminated with visible light and continuously stirred. During the process, 1 mL of the reaction solution was sampled at specific time intervals and filtered through a syringe filter (0.22 μm). The photocatalytic efficiency was monitored using high-performance liquid chromatography (HPLC) with a mobile phase of 70% methanol and 30% water.

Mechanistic investigations using radical trapping and ESR experiments for photodegradation of BPA.

Radical trapping experiments: The photocatalytic degradation of BPA under simulated sunlight was tested using a 300 W Xe lamp. Before the experiment, 5 mg of **CDP** and quantitative free radical capture agents were dispersed in 10 mL BPA (10 ppm). Then, an Xe lamp was used to irradiate the solution, and circulating water was used to keep the system temperature at room temperature to prevent the rapid solvent evaporation caused by overheating. Under the irradiation of the Xe lamp, aliquots of the suspension were taken at a certain time and filtered by syringe with a 0.22 μm filter for HPLC analyses.

ESR experiments: 10 mg of catalyst were dispersed in 5 mL pure water and sonicated for 15 min. For the detection of $\cdot O_2^-$, DMPO was used and prepared in 100

mM aqueous solution, and for the detection of $^1O_2$, TEMP was used and prepared in 100 mM aqueous solution. To a 5 mL brown glass vial, 200 µL of the catalyst suspension and 200 µL of DMPO/TEMP solution were mixed and sonicated for 5 min. The resulting suspension was then placed into a capillary and subjected to an ESR instrument for scanning for 50 seconds under both dark conditions and light conditions.

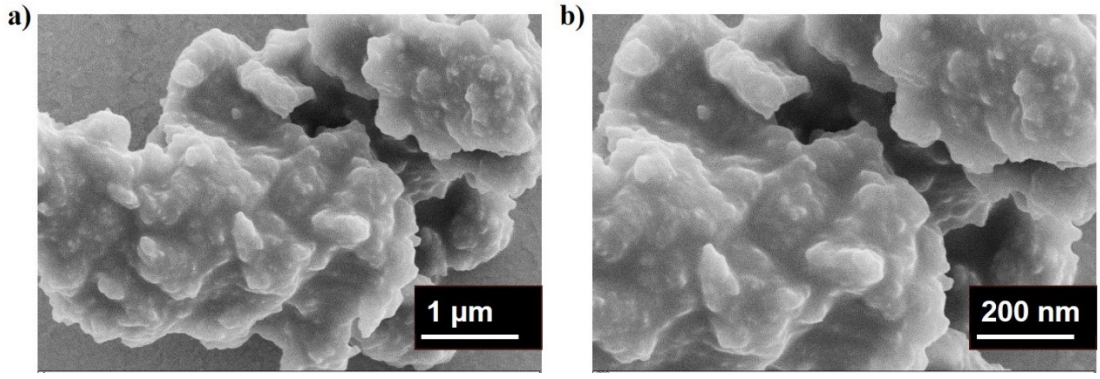

Fig. S13. a) and b) are SEM images of **CDP** catalyst after photocatalytic degradation reaction at 1 µm and 200 nm scale.

5. Others

Table S4. Comparison of efficiency of removing BPA by different catalysts.

Photocatalysts	**Catalyst dosage (g L^{-1})**	**BPA (ppm)**	**Degradation time (min)**	**Removal efficiency (%)**	**Light source**	**Reference**
SKA-CN	0.3	~10	100	98	300 W Xenon lamp	3
0.5 MB	0.5	10	180	87	300 W Xenon lamp	4
LCN	1	10	40	100	100 mW cm^{-2}, LED lamp	5
CTF-5Th/HSO_5^-	0.2	10	75	100	300 W Xenon lamp	6
STCH-COF_{10}	0.2	10	90	100	300 W Xenon lamp	7
Co-MiL-53-NH_2-BT	0.25	10	120	99.9	300 W Xenon lamp	8
SA-TCPP/O-CN-40%	0.5	10	480	70	500 W Xenon lamp	9
FePc/CN	0.1	10	130	50	250 W Xenon lamp	10
OCN 6	0.2	10	120	98.68	300 W	11

Traiazine-PDI	0.2	10	300	67	Xenon lamp 500 W Xenon lamp	[12]
PDINH	0.5	10	480	82	300 W Xenon lamp	[13]
g-C_3N_4	1	10	180	30	300 W Xenon lamp	[14]
CDP	**0.5**	**10**	**40**	**99**	**300 W Xenon lamp**	**This work**

References:

1. M. A. H. Alamiry, A. C. Benniston, J. Hagon, T. P. L. Winstanley, H. Lemmetyinen and N. V. Tkachenko, *RSC Adv.*, 2012*,* **2***,* 4944-4950.
2. X. Zheng, L. Zhang, M. Ju, L. Liu, C. Ma, Y. Huang, B. Wang, W. Ding, X. Luan and B. Shen, *ACS Appl. Mater. Interfaces*, 2022, **14**, 46262-46272.
3. L. Xu, L. Li, L. Yu and J. C. Yu, *Chem. Eng. J.*, 2022, **431**, 134241.
4. F. Chang, W. Yan, X. Wang, S. Peng, S. Li and X. Hu, *Chem. Eng. J.*, 2022, **428**, 131223.
5. F. Li, T. Li, L. Zhang, Y. Jin and C. Hu, *Appl. Catal. B, Environ.*, 2021, **296**, 120316.
6. S. Li, Z. Jin, X. Jiang, J. Yu, Y. Wang, S. Jin, H. Zhang, S. Song and T. Zeng, *Chem. Eng. J.*, 2022, **431**, 133900.
7. T. Zeng, Z. Jin, S. Li, J. Bao, Z. Huang, Y. Shen, H. Zhang, D. Wang and S. Song, *Chem. Commun.*, 2021, **57**, 4946-4949.
8. S.-W. Lv, J.-M. Liu, N. Zhao, C.-Y. Li, Z.-H. Wang and S. Wang, *J. Hazard. Mater.*, 2020, **387**, 122011.
9. J. Xu, Q. Gao, Z. Wang and Y. Zhu, *Appl. Catal. B, Environ.*, 2021, **291**, 120059.
10. T. Shi, H. Li, L. Ding, F. You, L. Ge, Q. Liu and K. Wang, *ACS Sustain. Chem. Eng.*, 2019, **7**, 3319-3328.
11. X. Long, C. Feng, S. Yang, D. Ding, J. Feng, M. Liu, Y. Chen, J. Tan, X. Peng, J. Shi and R. Chen, *Chem. Eng. J.*, 2022, **435**, 134835.
12. H. Zhang, X. Chen, Z. Zhang, K. Yu, W. Zhu and Y. Zhu, *Appl. Catal. B, Environ.*, 2021, **287**, 119957.
13. D. Liu, J. Wang, X. Bai, R. Zong and Y. Zhu, *Adv. Mater.*, 2016, **28**, 7284-7290.
14. L. Jing, D. Wang, M. He, Y. Xu, M. Xie, Y. Song, H. Xu and H. Li, *J. Hazard. Mater.*, 2021, **401**, 123309.